FORENSIC COSMOLOGY: PROBING BARYONS AND NEUTRINOS WITH BBN AND THE CBR

GARY STEIGMAN

Departments of Physics and Astronomy, The Ohio State University

Abstract. The primordial abundances of the light nuclides produced by Big Bang Nucleosynthesis (BBN) during the first 20 minutes in the evolution of the Universe are sensitive to the universal density of baryons and to the expansion rate of the early Universe. For example, while deuterium is an excellent baryometer, helium-4 provides an accurate chronometer. Some 400 kyr later, when the cosmic background radiation (CBR) was freed from the grasp of the ionized plasma of protons and electrons, the spectrum of temperature fluctuations also depended on (among other parameters) the baryon density and the density in relativistic particles. The comparison between the constraints imposed by BBN and those from the CBR reveals a remarkably consistent picture of the Universe at two widely separated epochs in its evolution. Combining these two probes leads to new estimates of the baryon density at present and tighter constraints on possible physics beyond the standard model of particle physics. In this review the consistency between these complementary probes of the universal baryon density and the early-Universe expansion rate is exploited to provide new constraints on any asymmetry between relic neutrinos and anti-neutrinos (neutrino degeneracy).

1 Introduction

As the hot, dense, early Universe expanded and cooled, it briefly evolved through the epoch of big bang nucleosynthesis (BBN), leaving behind the first complex nuclei: deuterium, helium-3, helium-4, and lithium-7. The abundances of these relic nuclides were fixed by the competition between the relative densities of nucleons (baryons) and photons (the baryon abundance) and the universal expansion rate. In particular, primordial deuterium is an excellent baryometer, while the relic abundance of ^{4}He provides an accurate chronometer. Some 400 thousand years later, when the cosmic background radiation (CBR) cooled sufficiently to allow neutral atoms to form, freeing the CBR from the embrace of the ionized plasma of protons and electrons, the spectrum of temperature fluctuations imprinted on the CBR recorded the baryon and radiation densities, along with the expansion rate of the Universe at that epoch. As a result, the relic abundances of the light nuclides and the CBR temperature fluctuation spectrum provide invaluable, complementary windows on the early evolution of the Universe and sensitive probes of its particle content.

In several, recent, related articles [1], the author has reviewed the current status of BBN and compared the BBN constraints on the baryon abundance and the early-Universe expansion rate with similar ones from the CBR (mainly from the WMAP data [2] and analyses [3]). In a nutshell, the BBN-inferred baryon density based on the relic abundance of deuterium is in near-perfect agreement with that derived from the CBR. Although the value of the primordial abundance of ^{4}He derived from observations of metal-poor (nearly primordial), extragalactic H II regions is low compared to the standard BBN (SBBN) prediction, suggesting a slower-than-standard early-Universe expansion rate, the SBBN prediction is within $\sim 2\sigma$ of the data and is entirely consistent with the weaker constraint on the expansion rate some 400 thousand years later provided by the CBR. This consistency of the standard model of cosmology permits the exploration of more exotic alternatives, one of which – a small but significant asymmetry between neutrinos and antineutrinos (neutrino degeneracy) – is explored here (see, also, Barger *et al.* (2003a) [4] and references therein).

To set the stage for the discussion of the cosmological constraints on neutrino degeneracy (see, e.g., Kang & Steigman 1992 [5]), we begin with a brief overview of SBBN and discuss the modifications to SBBN and the CBR in the presence of a non-standard, early-Universe expansion rate; for further details and references to related work, see Steigman (2003a,b,c) [1].

2 SBBN: An Overview

Discussion of BBN can begin when the Universe is a few tenths of a second old and the temperature is a few MeV. At such an early epoch the energy density is dominated by the relativistic (R) particles present and the universe is said to be "radiation-dominated" (RD). For sufficiently early times, when the temperature is a few times higher than the electron rest mass energy, these are photons, $e^{\pm}$ pairs and, for the standard model of particle physics, three flavors of left-handed (i.e., one helicity state) neutrinos (and their right-handed, antineutrinos). The hot, dense, early Universe is a hostile environment for complex nuclei. At sufficiently high temperatures ($T \gtrsim 80$ keV), when all the nucleons (baryons) were either neutrons or protons, their relative abundance was regulated by the weak interactions ($p + e^- \longleftrightarrow n + \nu_e$, $n + e^+ \longleftrightarrow p + \bar{\nu}_e$, $n \longleftrightarrow p + e^- + \bar{\nu}_e$); the higher mass of the neutron ensures that protons dominate (in the absence – for now – of a chemical potential for the electron-type neutrinos ν_e). Below ~ 80 keV, the Universe has cooled sufficiently that the cosmic nuclear reactor can begin in earnest, building the lightest nuclides D, ^{3}He, ^{4}He, and ^{7}Li. D and ^{3}He (also ^{3}H) are burned very rapidly to ^{4}He, the most tightly bound of the light nuclides. The absence of a stable mass-5 nuclide ensures that in the expanding, cooling, early Universe, the abundances of heavier nuclides are greatly suppressed. By the time the temperature has dropped below ~ 30 keV, a time comparable to the neutron lifetime, the average thermal energy of the nuclides and nucleons is too small to overcome the coulomb barriers, any remaining free neutrons decay, and BBN ceases.

Among the light nuclides synthesized during BBN the relic abundances of D, ^{3}He, and ^{7}Li are *rate limited*, determined by the competition between the reaction rates (which depend on the nucleon density) and the universal expansion rate. Any of these nuclides are potential baryometers. In the expanding Universe the number densities of all particles decrease with time, so that the magnitude of the baryon density (or that of any other particle) has no meaning without also specifying *when it is measured*. To quantify the universal abundance of baryons, it is best to compare the baryon number density $n_{\rm B}$ to the CBR photon number density n_γ. After $e^{\pm}$ pairs have annihilated the ratio of these number densities remains effectively constant as the Universe evolves. This ratio $\eta \equiv n_{\rm B}/n_\gamma$ is very small, so that it is convenient to define a quantity of order unity,

$$\eta_{10} \equiv 10^{10}(n_{\rm B}/n_\gamma) = 274\,\Omega_{\rm B}h^2 = 274\,\omega_{\rm B}, \tag{1}$$

where $\Omega_{\rm B}$ is the ratio (at present) of the baryon density to the critical density, h is the present value of the Hubble parameter in units of 100 km s^{-1} Mpc^{-1}, and $\omega_{\rm B} \equiv \Omega_{\rm B}h^2$. For SBBN, there is only one adjustable parameter, η (or $\omega_{\rm B}$).

As the post-$e^{\pm}$ annihilation Universe evolves, the ratio of nucleons (baryons) to photons is accurately preserved so that η at the time of BBN should be equal to its value at recombination (probed by the CBR) as well as its value today. Testing this over ten orders of magnitude in redshift, over a timespan of some 10 billion years, can provide a confirmation of the standard models of particle physics and of cosmology.

2.1 Deuterium – The BBN Baryometer of Choice

Deuterium is currently the baryometer of choice. As the Universe evolves, galaxies form, and gas is cycled through stars. As a consequence of its very weak binding, deuterium is burned at sufficiently low temperatures that it is completely destroyed in any gas which passes through stars. Therefore, in the post-BBN Universe the D abundance never exceeds its BBN value. Because the evolution of D is simple (no post-BBN sources), decreasing since BBN, observations of D anywhere, anytime, yield a *lower* bound to its primordial abundance. Observations of D in "young" systems (high redshift or low metallicity), should reveal a deuterium "plateau" at its primordial abundance. In addition to its simple post-BBN evolution, deuterium is the baryometer of choice also because its predicted primordial abundance ($y_{\rm D} \equiv 10^5(D/H)_{\rm P}$) is sensitive to the baryon density, $y_{\rm D} \propto \eta^{-1.6}$; as a result, a $\sim 10\%$ measurement of $y_{\rm D}$ will lead to a $\sim 6\%$ determination of η (or $\Omega_{\rm B}h^2$).

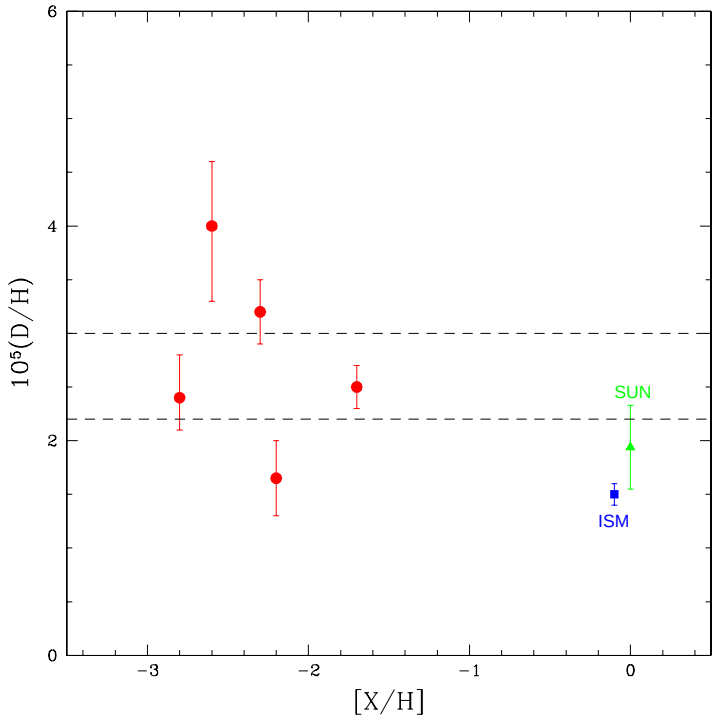

Figure 1: The deuterium abundance by number with respect to hydrogen versus the metallicity (relative to solar on a log scale), from observations (as of early 2003) of QSOALS (filled circles). Also shown for comparison are the D abundances for the local ISM (filled square) and the solar system ("Sun"; filled triangle). The dashed horizontal lines represent the range of the $\pm 1\sigma$ estimate for the primordial deuterium abundance ($y_{\rm D} = 2.6 \pm 0.4$) based on the QSOALS data.

In pursuit of the most nearly primordial value of the D abundance, it is best to concentrate on those systems which have experienced the least stellar evolution. Thus, while observations of D in the solar system and/or the local ISM provide useful *lower* bounds to the primordial D abundance, it is the observations of deuterium in a few high redshift, low metallicity, QSO absorption-line systems (QSOALS) which provide the most useful data. Presently there are only five QSOALS with reasonably firm deuterium abundance determinations [6]; the derived abundances of D are shown in Figure 1 along with the corresponding solar system and ISM D abundances.

As is clear from Figure 1, there is significant dispersion among the derived D abundances at low metallicity. The QSOALS data fail to reveal the anticipated deuterium plateau, suggesting that systematic errors may be present, contaminating some of the determinations of the D I and/or H I column densities. Since the D I and H I absorption spectra are identical, except for the wavelength/velocity offset resulting from the heavier reduced mass of the deuterium atom, an H I "interloper", a low-column density cloud shifted by ~ 81 km s^{-1} with respect to the main absorbing cloud, would masquerade as D I. If this is not accounted for, a D/H ratio which is too high would be inferred. Since there are more low-column density absorbers than those with high H I column densities, absorption-line systems with somewhat lower H I column density (e.g., Lyman-limit systems) are more susceptible to this contamination than are the higher H I column density absorbers (e.g., damped Lyα absorbers). It is intriguing that the two QSOALS with the highest D/H have the lowest H I column densities. In contrast, for the damped Lyα absorbers an accurate determination of the H I column density requires an accurate placement of the continuum, which could be compromised by interlopers. This might lead to an overestimate of the H I column density and a concomitant underestimate of D/H (J. Linsky, private communication). Again, it is intriguing that the lowest D/H is found for the system with the highest H I column density. Although these hints are suggestive, there is no observational evidence to support the exclusion of any of the current deuterium abundance determinations. Following the approach of O'Meara *et al.* [6] and Kirkman *et al.* [6], the weighted mean of the D abundances for the five lines of sight [6] is adopted for the primordial abundance, while the dispersion in the data is used to set the error: $y_{\rm D} = 2.6 \pm 0.4$. For the same data Kirkman *et al.* [6] derive a slightly higher mean

D abundance, $y_{\rm D} = 2.74$, by first finding the mean of $\log(y_{\rm D})$ and then using it to compute the mean D abundance ($y_{\rm D} \equiv 10^{\langle \log(y_{\rm D}) \rangle}$).

2.2 SBBN Baryon Density

For SBBN, the baryon density parameter corresponding to the primordial D abundance adopted here ($y_{\rm D} = 2.6 \pm 0.4$) is $\eta_{10} = 6.10^{+0.67}_{-0.52}$ ($\Omega_{\rm B} h^2 = \omega_{\rm B} = 0.0223^{+0.0024}_{-0.0019}$). This is in outstanding agreement with the Spergel *et al.* estimate [3] of $\Omega_{\rm B} h^2 = 0.0224 \pm 0.0009$ ($\eta_{10} = 6.14 \pm 0.25$), based largely on the new CBR (*WMAP*) data (Bennett *et al.* [2]). The concordance between SBBN and the CBR is spectacular.

In contrast to D, the post-BBN evolution of ^{3}He is complex. ^{3}He is destroyed in the hotter interiors of all but the least massive stars, while it survives in the cooler, outer layers of nearly all stars. Complicating the evolution of ^{3}He, hydrogen burning in low mass stars leads to the synthesis of significant amounts of *new* ^{3}He [7]. It is necessary to account for all of these effects quantitatively in the material returned by stars to the interstellar medium (ISM) if current Galactic data are to be used to infer the primordial ^{3}He abundance. In fact, current data [8] suggest that a very delicate balance exists between net production and net destruction of ^{3}He in the course of the evolution of the Galaxy, rendering difficult a precise estimate of the primordial abundance of ^{3}He. However, for the baryon density determined by D (or, the CBR), the SBBN-predicted abundance of ^{3}He is $y_3 = 1.0 \pm 0.1$, which may be compared to the outer-Galaxy abundance of $y_3 = 1.1 \pm 0.1$, suggested by Bania, Rood, & Balser [8] to be nearly primordial. This agreement between SBBN D and ^{3}He is excellent.

A similar scenario to that for ^{3}He may be sketched for ^{7}Li. As a weakly bound nuclide, it is easily destroyed when cycled through stars. The high lithium abundances observed in the "super-lithium-rich red giants" reveal that at least some stars can produce post-BBN lithium, but a key unsolved issue is how much of this newly-synthesized lithium is actually returned to the ISM. Furthermore, observations of nearly primordial lithium are limited to the oldest, most metal-poor stars in the Galaxy, stars that have had the most time to mix and destroy or dilute their surface lithium. To add to the uncertainties, errors in equivalent width measurements, in the temperature scales for the coolest Population II stars and, in their model atmospheres contribute to the overall error budget, accounting for at least some of the variations among the values of the primordial abundance of lithium inferred by different observers. For example, Ryan *et al.* (2000) [9] find $[{\rm Li}]_{\rm P} \equiv 12 + \log({\rm Li/H}) = 2.1$, while Bonifacio & Molaro (1997) and Bonifacio, Molaro, & Pasquini (1997) [9] derive $[{\rm Li}]_{\rm P} = 2.2$, and Thorburn (1994) and Bonifacio *et al.* (2002) [9] infer $[{\rm Li}]_{\rm P} = 2.3$. On the basis of these not entirely consistent estimates, the data suggest that $[{\rm Li}]_{\rm P} \approx 2.2 \pm 0.1$. However, for the baryon density fixed by SBBN the predicted relic abundance of lithium should be $[{\rm Li}]_{\rm P} \approx 2.65^{+0.09}_{-0.11}$. Compared to expectation, the observed lithium abundance is low. Either this is a challenge to SBBN or, more likely (see Pinsonneault *et al.* 2002 and further references therein [10]), a hint about nonstandard stellar astrophysics. At present the most promising approach is to use the observed and SBBN-predicted lithium abundances to learn about stellar evolution, rather than to use stellar observations to constrain the SBBN-inferred baryon density.

2.3 SBBN and ^{4}He

Unique among the relic nuclides, the primordial abundance (mass fraction) of ^{4}He is not rate limited, so that $Y_{\rm P}$ provides only a weak measure of η. The net effect on ^{4}He of post-BBN evolution was to burn hydrogen to helium, increasing the ^{4}He mass fraction above its primordial value ($Y > Y_{\rm P}$). Although there are solar system and ISM (Galactic H II regions) data for ^{4}He, the key to the $Y_{\rm P}$ determinations are the observations of ^{4}He in nearly unevolved, metal-poor regions. To date these are limited to the observations of helium and hydrogen recombination lines in extragalactic H II regions [11]. Unfortunately, the present H II region ^{4}He data lead to a very large dispersion in the derived $Y_{\rm P}$ values, ranging from $Y_{\rm P} = 0.234 \pm 0.003$ to $Y_{\rm P} = 0.244 \pm 0.002$, suggesting that current estimates may not be limited by statistics, but by uncorrected systematic errors [12]. Here, the compromise proposed by Olive, Steigman, and Walker [13] is adopted: $Y_{\rm P} = 0.238 \pm 0.005$; for further discussion and references, see Steigman (2003a,b,c) [1].

For ^{4}He there is tension between the data and SBBN. Given the very high accuracy of the SBBN-abundance prediction and the very slow variation of $Y_{\rm P}$ with η, the SBBN-predicted primordial abundance is tightly constrained: $Y_{\rm P}^{\rm SBBN} = 0.248 \pm 0.001$. Agreement with the adopted value of

$Y_P^{OSW} = 0.238 \pm 0.005$ (or, with the Izotov & Thuan [11] value of $Y_P^{IT} = 0.244 \pm 0.002$) is only at the $\sim 2\sigma$ level. This apparent challenge to SBBN provides an opportunity.

Recall that once BBN begins in earnest, essentially all available neutrons are incorporated into ^{4}He: Y_P is *neutron limited*. The neutron to proton ratio when BBN commences is determined by the competition between the weak interaction rates and the universal expansion rate, the latter of which is fixed in SBBN by the standard model particle content and the Friedman equation. However, if the early-Universe expansion rate differed from the standard model prediction, ^{4}He provides the ideal BBN chronometer with which to probe it. A slower expansion leaves fewer neutrons available to build ^{4}He, reducing the predicted value of Y_P.

The neutron-proton ratio at BBN can also be modified from its standard value by an *asymmetry* between the number densities of ν_e and $\bar{\nu}_e$ ("neutrino degeneracy"), described by a chemical potential μ_e (or, equivalently, by the dimensionless degeneracy parameter $\xi_e \equiv \mu_e/T$). For a *significant*, positive chemical potential ($\xi_e \gtrsim 0.01$; more ν_e than $\bar{\nu}_e$) there are fewer neutrons than for the "standard" case (SBBN), leading to the formation of less ^{4}He, reducing Y_P.

It is clear that if ^{4}He is paired with D (the BBN baryometer), together they can constrain cosmological models with nonstandard expansion rates (or particle content) or neutrino degeneracy. After reviewing the BBN and CBR constraints on models with nonstandard, early-Universe expansion rates (see Steigman 2003a,b,c [1] and further references therein), this review concentrates on using BBN and the CBR to constrain any neutrino degeneracy (see Barger *et al.* 2003a [4] for further details and references to related work).

3 Early Universe Expansion Rate

The expansion rate (measured by the Hubble parameter H) is related to the energy density through the Friedman equation ($H^2 = \frac{8\pi G}{3}\rho$). During BBN the Universe is "radiation-dominated" (RD); the energy density (ρ_R) dominated by the relativistic particles present. For the standard model (SBBN) there are three families of light (relativistic) neutrinos ($N_\nu = 3$). For models with nonstandard, early-Universe expansion rates it is convenient to introduce the *expansion rate factor* $S \equiv H'/H = t/t'$. One possible origin for a nonstandard expansion rate ($S \neq 1$) is a modification of the energy density by the presence of "extra" relativistic particles X: $\rho_R \to \rho'_R = \rho_R + \rho_X$. If the additional energy density is normalized to that which would be contributed by additional flavors of (decoupled) neutrinos (Steigman, Schramm, & Gunn [14]), $\rho_X \equiv \Delta N_\nu \rho_\nu$, and $N_\nu = 3 + \Delta N_\nu$. It must be emphasized that the fundamental physical parameter is S, the expansion rate factor, which may be related to ΔN_ν (*nonlinearly*) by

$$S_{pre} \equiv (H'/H)_{pre} = (1 + 0.163\Delta N_\nu)^{1/2}\,; \;\; S_{post} \equiv (H'/H)_{post} = (1 + 0.135\Delta N_\nu)^{1/2}, \qquad (2)$$

where the subscripts "*pre*" and "*post*" reflect the values prior to, and after $e^\pm$ annihilation, respectively. However, any term in a modified Friedman equation which scales like radiation (decreases as the fourth power of the scale factor), such as may be due to higher dimensional effects as in the Randall-Sundrum [15] model, will change the standard-model expansion rate ($S \neq 1$) and may be related to an *equivalent* ΔN_ν (which could be *negative* as well as positive; $S > 1$ and $S < 1$ are both possible) through Eq. 2.

3.1 BBN Constraints on S

The qualitative effects of a nonstandard expansion rate on the relic abundances of the light nuclides may be understood as follows. For the baryon abundance range of interest ($1 \lesssim \eta_{10} \lesssim 10$) the relic abundances of D and ^{3}He are decreasing functions of η, revealing that in this range D and ^{3}He are being destroyed. A faster than standard expansion ($S > 1$) leaves less time for destruction, so more D and ^{3}He survive. At the higher values of η suggested by D, the ^{7}Li abundance increases with η, so that less time available ($S > 1$) results in less production and a *smaller* ^{7}Li relic abundance. Generally, these effects on the relic abundances of D, ^{3}He, and ^{7}Li are subdominant to their dependences on the baryon density. Not so for ^{4}He, whose relic abundance is weakly (logarithmically) dependent on the baryon density, while being strongly affected by the early-Universe expansion rate. A faster expansion leaves more neutrons available to be incorporated into ^{4}He; to a good approximation, ΔY

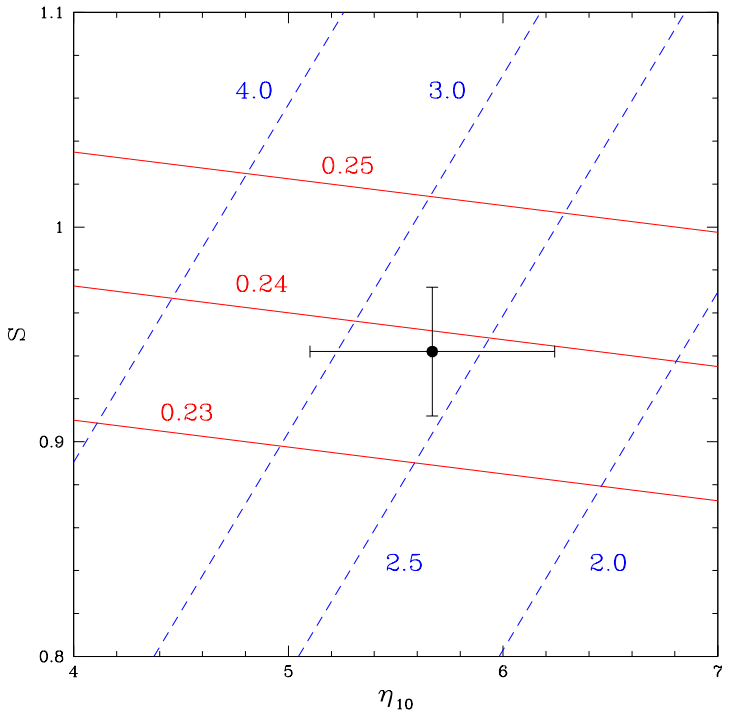

Figure 2: Isoabundance curves for D and ^{4}He in the expansion rate parameter (S) – baryon abundance parameter (η_{10}) plane. The dashed curves are for the deuterium abundances; the numbers are the values of $y_{\rm D} \equiv 10^5$(D/H). The solid curves are for the helium-4 mass fractions; the numbers correspond to $\rm Y_P$. The filled circle with error bars is for the adopted D and ^{4}He abundances (see the text).

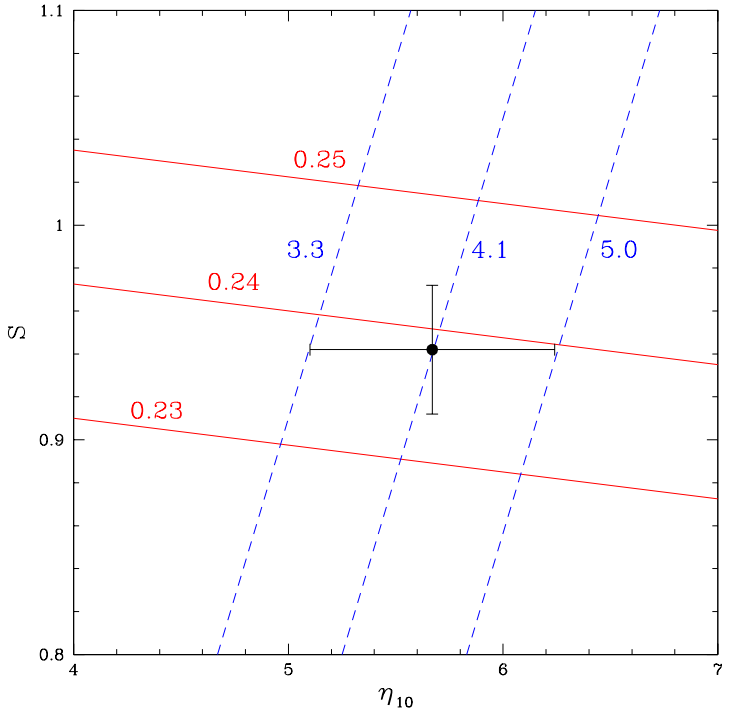

Figure 3: Isoabundance curves for ^{7}Li and ^{4}He in the expansion rate parameter (S) – baryon abundance parameter (η_{10}) plane. The dashed curves are for the lithium abundances; the numbers are the values of $y_7 \equiv 10^{10}$(Li/H). The solid curves are for the helium-4 mass fractions; the numbers correspond to $\rm Y_P$. The filled circle with error bars is for the adopted D and ^{4}He abundances (see the text).

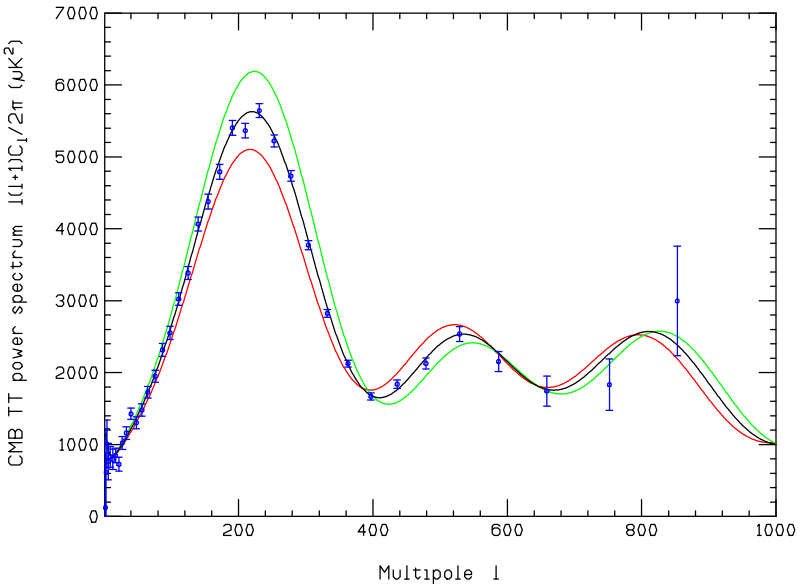

Figure 4: The CBR temperature fluctuation anisotropy spectra for three choices of the baryon density parameter $\omega_{\rm B} = 0.018$, 0.023, 0.028, in order of increasing height of the first peak. The WMAP data points [2] are shown.

$\approx 0.16\,(S-1)$. Using D as our baryometer and ^{4}He as our chronometer, the BBN constraints on η and S are shown in the $S-\eta$ plane in Figure 2, employing approximations to the D and ^{4}He isoabundance contours [16] which are typically good to a few percent or better.

It is clear from Figure 2 that the adopted D and ^{4}He abundances favor a slower-than-standard expansion rate. The best fit point is at $S = 0.94$ ($\Delta {\rm N}_\nu = -0.7$). However, the 2σ range in N_ν extends from $N_\nu = 1.7$ to $N_\nu = 3.0$, consistent with the standard case of $N_\nu = 3$.

In Figure 3 are shown the corresponding ^{7}Li – ^{4}He isoabundance contours in the $S-\eta$ plane, along with the best fit point and 1σ error from the adopted D and ^{4}He abundances. The constraints on S and η derived from D and ^{4}He lead to a predicted primordial lithium abundance in the range $2.5 \lesssim [{\rm Li}]_{\rm P} \lesssim 2.7$, not very different from the range for SBBN. It is clear that BBN with a nonstandard expansion rate, consistent with D and ^{4}He, cannot relieve the tension between the BBN-predicted ^{7}Li abundance and that inferred from metal-poor stars in the Galaxy. As mentioned earlier (§2.2), the solution likely lies with the stellar astrophysics.

3.2 Joint BBN and CBR Constraints on S and $\omega_{\rm B}$

The CBR temperature anisotropy and polarization spectra are sensitive to the baryon density and to the early-Universe (RD) expansion rate (see, e.g., Barger *et al.* (2003b) [17], and references to related work therein). Increasing the baryon density increases the inertia of the baryon-photon fluid, shifting the positions and the relative sizes of the odd and even acoutic peaks; see Figure 4. Changing the expansion rate (or, the relativistic particle content) changes the redshift of matter-radiation equality, also shifting the locations of the peaks. Since any change in ΔN_ν (or S) can be mimicked by a corresponding change in the total matter density $w_{\rm M} \equiv \Omega_{\rm M} h^2$, there is a degeneracy in the CBR anisotropy spectrum between S and $w_{\rm M}$ which can be broken using the HST Key Project determination of the Hubble parameter [17]. CBR temperature anisotropy spectra for four choices of N_ν are shown in Figure 5. Although the CBR temperature anisotropy spectrum is a less sensitive early-Universe chronometer than is BBN (^{4}He), the WMAP data may be used to identify allowed regions in the ΔN_ν (or S) – η plane, similar to those from BBN using D and ^{4}He. There is excellent overlap between the η – ΔN_ν (S) likelihood contours from BBN and those from the CBR (see Barger *et al.* (2003b) [17]); this variant of SBBN ($S \neq 1$) is consistent with the CBR. In Figure 6 (from Barger *et al.* (2003b) [17]) the confidence contours in the η – ΔN_ν plane are shown for a joint BBN – CBR fit. Although the best fit value for ΔN_ν is negative (driven largely by the adopted value for ${\rm Y_P}$), the standard-model value of $\Delta N_\nu = 0$ ($S = 1$) is quite acceptable.

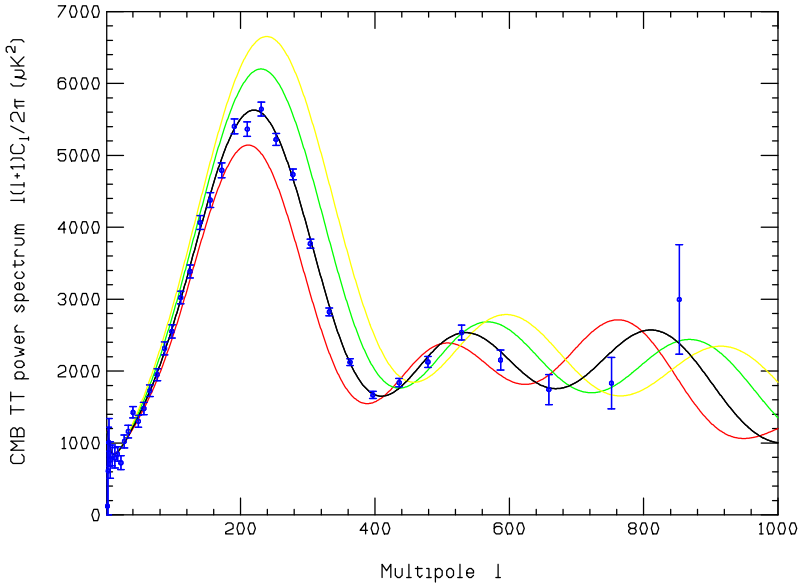

Figure 5: The CBR temperature fluctuation anisotropy spectra for four choices of $N_\nu = 1$, 2.75, 5, 7, in order of increasing height of the first peak. The WMAP data points [2] are shown.

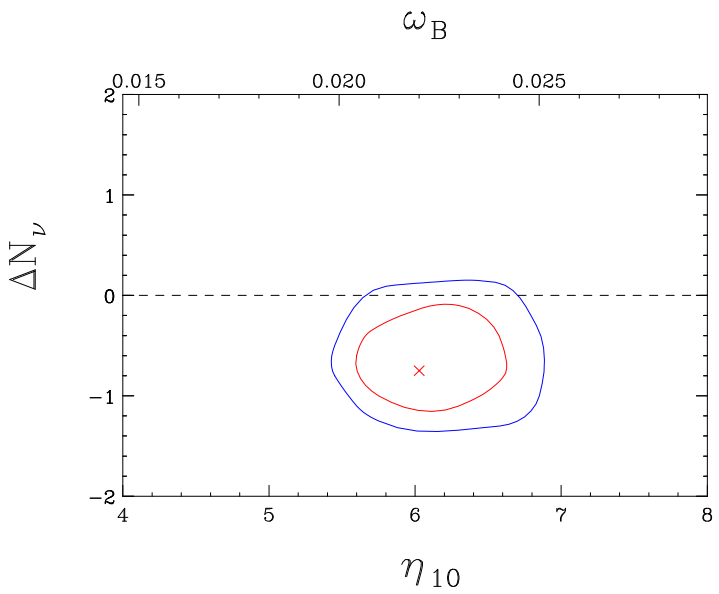

Figure 6: The 1σ and 2σ contours in the η ($\omega_{\rm B}$) – ΔN_ν plane for the joint BBN – CBR (*WMAP*) fit.

4 Neutrino Asymmetry

Oscillations among the three known (active) neutrinos (ν_e, ν_μ, ν_τ) will equilibrate any pre-existing asymmetries in any (all) of them to the level of the electron neutrino degeneracy prior to BBN [18]. Thus, the magnitude of the electron neutrino degeneracy allowed by BBN (and the CBR) is of special interest to any determination of constraints on the universal lepton asymmetry. As will be seen below (see Barger *et al.* (2003a) [4]), the BBN constraints provide the limit $\xi_e \approx \xi_\mu \approx \xi_\tau \lesssim 0.3$. This constraint is important because *any* neutrino degeneracy ($\xi_e >$ or < 0) implies a higher energy density in the relic neutrinos compared to the standard, $\xi_e = 0$ (or, $|\xi_e| \ll 1$) case; for the three active neutrinos with $\xi_e = \xi_\mu = \xi_\tau \lesssim 0.3$, the extra energy, expressed in terms of an equivalent number of extra neutrinos, is limited to $\Delta N_\nu \approx \frac{90}{7}(\frac{\xi_e}{\pi})^2 \lesssim 0.1$. As a result, the effect of neutrino degeneracy on the CBR, limited to its effect on S, is quite small. Thus, while BBN and the CBR are both sensitive to the baryon density and the expansion rate, only BBN is sensitive to the range of neutrino degeneracy of interest. Therefore, the CBR can provide independent constraints on S and η, allowing BBN to be used to limit neutrino degeneracy.

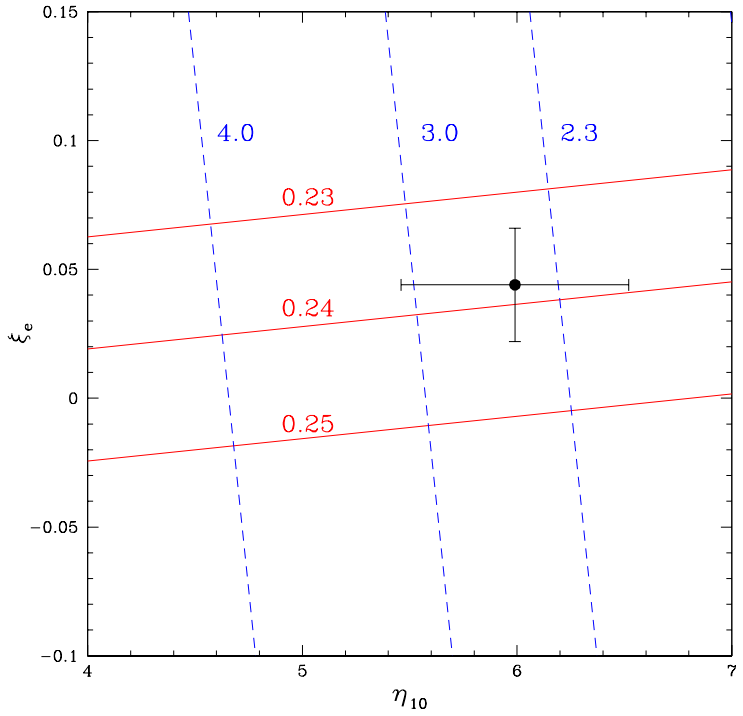

Figure 7: Isoabundance curves for D and ^{4}He in the neutrino asymmetry parameter (ξ_e) – baryon abundance parameter (η_{10}) plane. As in Fig. 2, the dashed curves are for the deuterium abundances and the solid curves are for the helium-4 mass fractions. The filled circle with error bars is for the adopted D and ^{4}He abundances.

4.1 BBN and ξ_e

As discussed in §2.3, Y_P is sensitive to any neutrino asymmetry. More ν_e than $\bar{\nu}_e$ drives down the neutron-to-proton ratio, leaving fewer neutrons available to build ^{4}He; to a good approximation $\Delta Y \approx -0.23\,\xi_e$ [5]. In contrast, the relic abundances of D, ^{3}He, and ^{7}Li are very insensitive to $\xi_e \neq 0$, so that when paired with ^{4}He, they can simultaneously constrain the baryon density and the electron-neutrino asymmetry. In analogy with Figures 2 and 3 for S versus η, in Figures 7 and 8 are shown the approximate D – ^{4}He and ^{7}Li – ^{4}He isoabundance curves [16] in the $\xi_e - \eta_{10}$ plane for the case where the expansion rate is fixed at its standard value, $S = 1$.

While the best fit point is at a non-zero neutrino aysmmetry, $\xi_e = 0.044$ (and $\eta_{10} = 6.0$), $\xi_e = 0$ is consistent at the $\sim 2\sigma$ level (and $\xi_e \gtrsim 0.09$ is excluded at $\sim 2\sigma$). It is clear from Figure 8 that the combination of neutrino asymmetry and baryon density which reconciles D and ^{4}He, leaves the BBN-predicted ^{7}Li abundance virtually unchanged from its SBBN value; the BBN-predicted ^{7}Li abundance is still too large compared to that inferred from the metal-poor halo stars in the Galaxy.

5 Joint BBN and CBR Constraints on ξ_e

Now consider the case where *both* ξ_e and ΔN_ν (S) are free to vary. As N_ν increases, so too will the best fit values of η and ξ_e. If N_ν increases, the early universe expands more rapidly, leaving *less* time to burn D. As a result, for a *fixed* baryon density parameter y_D *increases*. To reduce y_D back to its observed value, the baryon density parameter must increase. But, the combination of an increased baryon-to-photon ratio and $N_\nu > 3$, raises the predicted primordial abundance of ^{4}He, requiring a larger ξ_e to reconcile the BBN predictions with the data. For *any* (reasonable) choice of N_ν there is always a pair of $\{\eta_{10}, \xi_e\}$ values for which *perfect* agreement with the observed D and ^{4}He abundances can be obtained. It is, of course, not surprising that with three parameters and two constraints, such a fit can be found. Another observational constraint is needed to break this degeneracy and to simultaneously constrain η, S, and ξ_e. While neither ^{3}He nor ^{7}Li can provide the needed constraint, the CBR temperature anisotropy spectrum, which is sensitive to η and S but not to ξ_e, can (see Barger

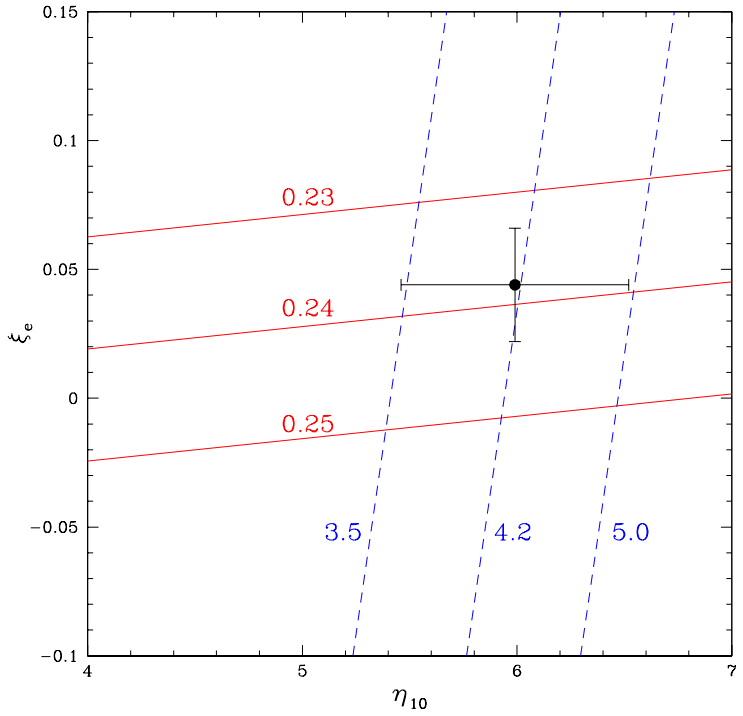

Figure 8: Isoabundance curves for ^{7}Li and ^{4}He in the neutrino asymmetry parameter (ξ_e) – baryon abundance parameter (η_{10}) plane. As in Fig. 3, the dashed curves are for the lithium abundances and the solid curves are for the helium-4 mass fractions. The filled circle with error bars is for the adopted D and ^{4}He abundances.

et al. 2003a [4]).

With the primordial abundances of D and ^{4}He as fixed constraints, increased values of ξ_e may be compensated by increased values of ΔN_ν and η. This degeneracy is broken by the WMAP CBR data which provides restrictions on the relation between ΔN_ν and η. The expanded ranges of ξ_e and ΔN_ν which are consistent with both the CBR and BBN are shown in Figure 9. Values of ΔN_ν in the range $-2 \lesssim \Delta N_\nu \lesssim 5$ are allowed, *provided that* the neutrino asymmetry parameter lies in the range $-0.1 \lesssim \xi_e \lesssim 0.3$ (and, vice-versa). While permitting three free parameters (η, ΔN$_\nu$, ξ_e) weakens the constraints on any one of them, the *combination* of BBN and the CBR can provide meaningful bounds. Allowing nonzero values of ξ_e weakens the previous BBN restrictions (§3.1) on ΔN_ν (or, on the early-Universe expansion rate parameter S). Nonetheless, after marginalizing over ξ_e, the 95% confidence level range for ΔN_ν is $-1.7 \lesssim \Delta N_\nu \lesssim 4.1$ (Barger *et al.* (2003a) [4]).

6 Conclusions

For the standard models of cosmology and particle physics, the SBBN-predicted primordial abundances of D, ^{3}He, ^{4}He, and ^{7}Li depend on only one free parameter, the baryon abundance parameter. Of the light nuclides, deuterium is the baryometer of choice; the SBBN-derived baryon density based on D, η_{10}(SBBN) $= 6.10^{+0.67}_{-0.52}$, is in excellent (exact!) agreement with that derived from non-BBN, mainly CBR, data (Spergel *et al.* (2003) [3]): η_{10}(CBR) $= 6.14 \pm 0.25$. Unique among the relic nuclides, ^{4}He is an excellent chronometer and is also sensitive to any $\nu_e - \bar{\nu}_e$ asymmetry. While for SBBN the predicted primordial ^{4}He mass fraction is slightly low compared to available data, the uncertainties in the observationally inferred primordial value are likely dominated by systematics. However, if the tension between SBBN D and ^{4}He persists, it could be relieved by a nonstandard expansion rate, by a neutrino asymmetry, or by both acting together. Neither of these options can reconcile the BBN prediction with the low abundance of lithium inferred from observations of metal-poor stars, suggesting that the resolution of this conflict is likely to be found in the stellar astrophysics [10]. Taken together, the CBR (WMAP) and BBN (D & ^{4}He) are consistent with $\eta_{10} \approx 6$ ($\omega_{\rm B} \approx 0.022$) and (for $\xi_e \equiv 0$) $1.7 \leq$ N$_\nu \leq 3.0$, or (for $S \equiv 1$) $0 \lesssim \xi_e \lesssim 0.09$ (both at $\sim 2\sigma$). For both ΔN_ν and ξ_e free, $1 \lesssim$ N$_\nu \lesssim 7$ and $-0.1 \lesssim \xi_e \lesssim 0.3$ are permitted by the joint BBN and CBR data.

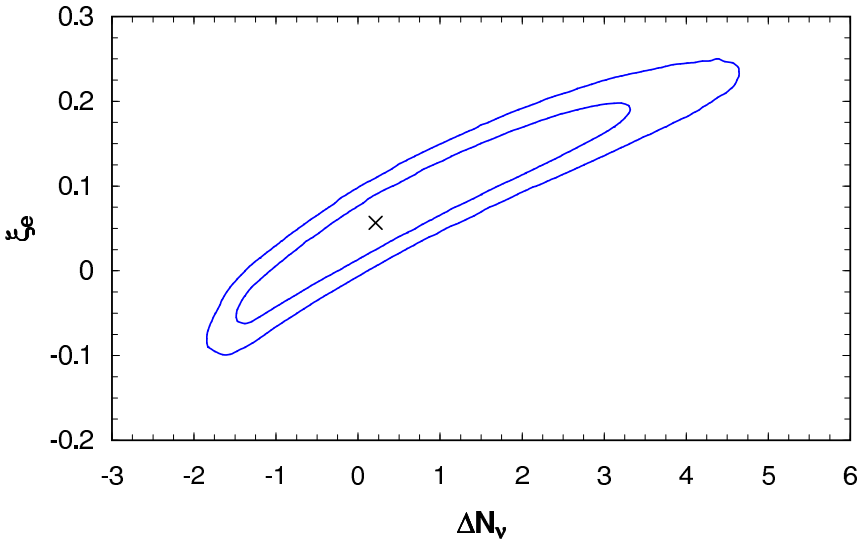

Figure 9: The 1σ and 2σ contours in the ΔN_ν – ξ_e plane using WMAP data and BBN with the adopted D and ^{4}He abundances. The best-fit point is marked with a cross.

In the current, data-rich era of cosmological research, BBN continues to play an important role. The spectacular agreement among the estimates of the baryon density inferred from processes occurring at widely separated epochs confirms the general features of the standard models of cosmology and of particle physics. Although there have been many successes, much remains to be done. Whether the resolutions of the current challenges are observational or theoretical, cosmological or astrophysical, the future is bright.

Acknowledgements. I am grateful to all my collaborators, past and present, and I thank them for their contributions to the material reviewed here. Many of the quantitative results (and figures) presented here are from recent collaborations or discusions with V. Barger, J.P. Kneller, D. Marfatia, K.A. Olive, R.J. Scherrer, and T.P. Walker. My research is supported at OSU by the DOE through grant DE-FG02-91ER40690. This manuscript was prepared while I was visiting the Instituto Astrônomico e Geofísico of the Universidade de São Paulo; I thank them for their hospitality.

References

[1] Steigman, G., 2003a, Big Bang Nucleosynthesis: Probing The First 20 Minutes, To appear in the Carnegie Observatories Astrophysics Series, Vol. 2: Measuring and Modeling the Universe; ed. W. L. Freedman (Cambridge: Cambridge University Press) (astro-ph/0307244); Steigman, G., 2003b, Primordial Nucleosynthesis, To appear in the Proceedings of the May 2003 STScI Symposium, "The Local Group As An Astrophysical Laboratory"; ed. M. Livio (Cambridge: Cambridge University Press) (astro-ph/0308511); Steigman, G., 2003c, The Baryon Budget From BBN And The CBR, To appear in the proceedings of the XV Rencontres de Blois, "Physical Cosmology: New Results in Cosmology and the Coherence of the Standard Model" (astro-ph/0309338)

[2] Bennett, C. L. *et al.*, 2003, Astrophys. J. Suppl., 148, 1.

[3] Spergel, D. N. *et al.*, 2003, Astrophys. J. Suppl., 148, 175.

[4] Barger, V., Kneller, J. P., Marfatia, D., Langacker, P. & Steigman, G., 2003a, Phys. Lett. B, 569, 123.

[5] Kang, H.-S. & Steigman, G., 1992, Nucl. Phys. B., 372, 494.

[6] Burles, S. & Tytler, D., 1998a, Astrophys. J., 499, 699; *ibid*, Astrophys. J., 507, 732; O'Meara, J. M., Tytler, D., Kirkman, D., Suzuki, N., Prochaska, J. X., Lubin, D., & Wolfe, A. M., 2001,

Astrophys. J., 552, 718; Pettini M. & Bowen, D. V., 2001, Astrophys. J., 560, 41; Kirkman, D., Tytler, D., Suzuki, N., O'Meara, J. M., & Lubin, D., 2003, Astrophys. J. Suppl., submitted (astro-ph/0302006).

[7] Iben, I. I., 1967, Astrophys. J., 147, 624; Rood, R. T., 1972, Astrophys. J., 177, 681; Rood, R. T., Steigman, G. & Tinsley, B. M., 1976, Astrophys. J. Lett., 207, L57; Dearborn, D. S. P., Schramm, D. N., & Steigman, G., 1986, Astrophys. J., 203, 35.

[8] Bania, T. M., Rood, R. T., & Balser, D., 2002, Nature, 415, 54.

[9] Thorburn. J. A., 1994, Astrophys. J., 421, 318; Bonifacio, P. & Molaro, P., 1997, MNRAS, 285, 847; Bonifacio, P., Molaro, P., & Pasquini, L., 1997, MNRAS, 292, L1; Ryan, S. G., Beers, T. C., Olive, K. A., Fields, B. D., & Norris, J. E., 2000, Astrophys. J. Lett., 530, L57; Bonifacio, P., *et al.*, 2002, Astron. & Astrophys., 390, 91.

[10] Pinsonneault, M. H., Steigman, G., Walker, T. P., & Narayanan, V. K., 2002, Astrophys. J., 574, 398.

[11] Olive, K. A. & Steigman, G., 1995, Astrophys. J. Suppl., 97, 49; Izotov, Y. I., Thuan T. X. & Lipovetsky V. A., 1997, Astrophys. J. Suppl., 108, 1; Olive, K. A., Skillman, E., & Steigman, G., 1997, Astrophys. J., 483, 788; Izotov, Y. I. & Thuan, T. X., 1998, Astrophys. J., 500, 188.

[12] Viegas, S. M., Gruenwald, R., & Steigman, G., 2000, Astrophys. J., 531, 813.

[13] Olive, K. A., Steigman, G., & Walker, T. P., 2000, Phys. Rep., 333, 389.

[14] Steigman, G., Schramm, D. N., & Gunn, J. E., 1977, Phys. Lett. B, 66, 202.

[15] Randall, L. & Sundrum, R., 1998a, Phys. Rev. Lett., 83, 3370; *ibid*, 1998b, Phys. Rev. Lett., 83, 4690; Binetruy, P., Deffayet, C., Ellwanger, U., & Langlois, D., 2000, Phys. Lett. B, 477, 285; Cline, J. M., Grojean, C., & Servant, G., 2000, Phys. Rev. Lett., 83, 4245.

[16] Kneller, J. P. & Steigman, G., 2003, BBN For Pedestrians, In preparation.

[17] Barger, V., Kneller, J. P., Lee, H.-S., Marfatia, D., & Steigman, G., 2003b, Phys. Lett. B, 566, 8.

[18] Lunardini, C. & Smirnov, A. Y., 2001, Phys. Rev. D, 64, 073006; Dolgov, A. D., Hansen, S. H., Pastor, S., Petcov, S. T., Raffelt, G. G., & Semikoz, D. V., 2002, Nucl. Phys. B, 632, 363; Abazajian, K. N., Beacom, J. F., & Bell, N. F., 2002, Phys. Rev. D, 66, 013008; Wong, Y. Y. 2002, Phys. Rev. D, 66, 025015.